ACS OMEGA

http://pubs.acs.org/journal/acsodf

Article

Synergistic Effect of Multifunctional Layered Double Hydroxide-Based Hybrids and Modified Phosphagen with an Active Amino Group for Enhancing the Smoke Suppression and Flame Retardancy of Epoxy

Xiang Chen,[‖] Bingyi Wang,[‖] Zhifeng Hao,* Guizhen Tan, Mohamed S. Selim, Jian Yu, and Yingmin Huang*

Cite This: *ACS Omega* 2022, 7, 21714−21726

Read Online

ACCESS | Metrics & More | Article Recommendations | Supporting Information

ABSTRACT: To improve the fire hazard of epoxy resin (EP), phosphomolybdate (PMoA), as a classical Keggin cluster, was successfully intercalated into Mg, Al, and Zn layered double hydrotalcite (LDH) by the reconstruction method, and it was denoted as MgAlZn-LDH-PMoA. The structure and morphology of MgAlZn-LDH-PMoA were characterized by X-ray diffraction and Fourier transform infrared spectroscopy. Subsequently, hexa(4-aminophenoxy)cyclotriphosphazene (HACP) was prepared and characterized as a high-performance organic flame retardant, which is rich in flame elements phosphorus and nitrogen. The synergistic effects of MgAlZn-LDH-PMoA and HACP on the fire safety of EP composites loaded with different amounts of flame retardant hybrids were studied in detail. Thermogravimetric analysis showed that the char residue of these EP composites increased significantly. Compared with the EP matrix filled with only MgAlZn-LDH-PMoA or HACP, the incorporation of MgAlZn-LDH-PMoA and HACP had a synergistic effect on promoting char formation of EP composites. Particularly, the char yield of EP7 is as high as 29.0%. Furthermore, the synergistic effects of incorporation of MgAlZn-LDH-PMoA with HACP were investigated using the cone calorimeter combustion tests. The results showed that the total heat release and peak heat release rate of the EP composites remarkably declined by 35.2 and 50.9%, respectively, with a loading of 7 wt % hybrid flame retardant. Moreover, the hybrid flame retardants also showed an obvious inhibitory effect on the total smoke production and the release of toxic CO gas. The detailed analysis of the residual char indicated that the main mechanism for improving the flame retardancy and smoke suppression performance is due to both the catalytic carbonization of MgAlZn-LDH-PMoA and phosphoric acid compounds and physical barrier function of the char layer. In addition, the molybdenum oxides produced from $[PMo_{12}O_{40}]^{3-}$ during combustion can not only increase the yield and compactness of the char layer but also reduce the release of CO through a redox reaction, which has important application value to reduce the fire hazard.

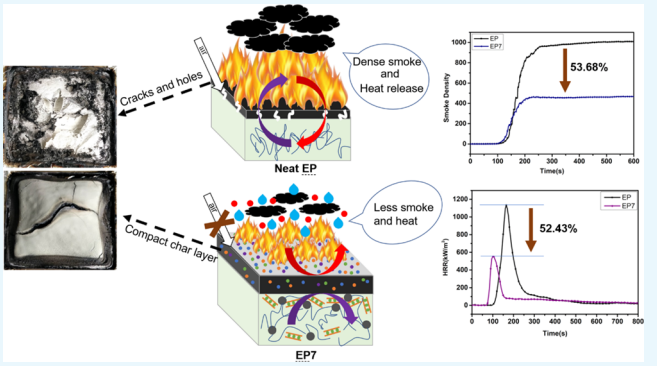

1. INTRODUCTION

Epoxy resin (EP) is one of the most important industrial thermosetting polymers and is widely used in aerospace, electric products, coatings, composite matrix, and other fields, owing to the excellent chemical stability, good mechanical stiffness, and dielectric properties.[1,2] Unfortunately, the structural composition of the carbon−hydrogen chain of EP makes it extremely flammable in the air, accompanied by the production of dense smoke and combustible gases. The flammability of EP not only limits its further application but also poses a serious threat to the lives and property of people.[3,4] In recent decades, halogenated flame retardants have been used extensively because of their excellent flame retardant effect on polymers. However, their adverse effects to the environment and human health in the process of combustion have directed modern research toward halogen-free and environmental-friendly flame retardants.[5,6] Therefore, it is imperative to adopt a creative method of smoke suppression and environmental protection to reduce the fire risk of EP.

As an important part of two-dimensional nanomaterials, Mg and Al layered double hydroxide (LDH) has attracted great

Received: March 22, 2022
Accepted: June 3, 2022
Published: June 16, 2022

interest recently because of its high specific surface area, good endothermic absorption performance, excellent carbonization properties, and smoke suppression properties.[7,8] However, the high polarity of LDHs weakens their surface interaction with the polymer matrix, thus affecting their dispersion in the matrix. Moreover, it is usually necessary to achieve better flame retardancy by high LDH loadings, which weakens the mechanical properties of the polymer. To overcome this problem, some researchers used functional anions to modify LDHs, such as dodecyl benzene sulfonate, borate, and phosphates,[9−11] which could enhance the dispersibility and flame retardation of LDHs in the polymer matrix. Furthermore, this route has become an important strategy to develop advanced flame retardant materials.

At present, there are many reports about effective flame retardants for the EP resin matrix, but there are few reports on halogen-free nanostructured materials that show both the function of flame retardancy and smoke suppression. The release of toxic gases (such as CO) from flammable substances during combustion in confined spaces causes great harm to our human health. Accordingly, it is of great importance to develop novel multiple functional flame retardants. Xu et al. reported a hybrid RGO-LDH/$CuMoO_4$ by introducing $CuMoO_4$ onto the surface of two-dimensional nanostructured RGO-LDH. The study of its effect on flame retardancy and smoke suppression showed that the smoke density and total heat release (THR) of the composite with 2 wt % RGO-LDH/$CuMoO_4$ addition significantly decreased compared with those of pure EP. This is mainly due to the formation of MoO_3 and Cu_2O generated from RGO-LDH/$CuMoO_4$ during the combustion process, which promotes the formation of more char and improves the compactness of the char layer.[12] Wang et al. prepared a hybrid material MWCNT-MoS_2 by electrostatic interaction and mixed it with the EP matrix to improve its combustion performance. Their study indicated that the addition of 2 wt % MWCNT-MoS_2 into EP improved the flame retardancy significantly and reduced the maximum peak heat release rate (PHRR) by 43.3%. The results showed that MoS_2 can form a large barrier network, inhibiting the effusion of pyrolytic products and then decreasing the heat release of surface combustion.[13] The latest studies show that the design and synthesis of novel compounds containing Mo are an effective means to obtain multifunctional flame retardants. In consideration of the fact, phosphorus is also an effective flame retardant element.[14−17] Our strategy for improving the flame retardancy of LDH is to insert negatively charged $PMo_{12}O_{40}^{3-}$ into the positively charged laminates of LDHs by the reconstruction method. With this creative strategy, there is no doubt that the dispersion of LDHs in the EP matrix will be improved by intercalation. On the other hand, the flame retardant elements molybdenum and phosphorus present in $PMo_{12}O_{40}^{3-}$ through cooperation with the two-dimensional layered nanomaterial LDHs will improve the multifunctional performance of the hybrid materials, both for flame retardancy and smoke suppression.[18,19]

In the process of the development of novel flame retardants, the preparation of cyclotriphosphonitrile flame retardants from hexachlorocyclotriphosphazene (HCCP) has been widely valued by researchers because of its special phosphorus and nitrogen skeleton structure.[20,21] Recently, cyclotriphosphonitrile compounds containing phenoxy, ethylene oxide, and other functional groups have been successfully synthesized and applied as flame retardant polymers.[22−25] The flame retardancy mechanism can be roughly summed up as follows. First, the phosphate, metaphosphate, and polyphosphate produced during the high-temperature pyrolysis of cyclotriphosphazene compounds can promote the carbonization of the polymer effectively. Also, the nonvolatile protective film formed can adhere to the polymer surface and reduce heat transfer and the entry of oxygen. Second, the noncombustible gases, for instance, CO_2, N_2, and NH_3, released during combustion can dilute oxygen and combustible pyrolysis gas so as to achieve a good flame retardant effect.[26,27] However, cyclotriphosphazene compounds are poorly compatible with polymers and can easily absorb moisture, so it is difficult to use them in engineering. Thus, our creative strategy is to synthesize a functional cyclotriphosphazene compound that has an active amino group. At high temperatures, the active amino group in the cyclotriphosphazene compound can react with the epoxy group in EP, which not only improves the compatibility between the EP matrix and the flame retardant but also plays the role of curing and reduces the amount of curing agent.

In this study, the compound MgAlZn-LDH-CO_3 was prepared by the coprecipitation method first and then the classical Keggin cluster of phosphomolybdate ($PMo_{12}O_{40}^{3-}$) was intercalated into the interlayer space of LDHs by the reconstruction method to obtain the multifunctional LDH hybrid MgAlZn-LDH-PMoA. In addition, cyclotriphosphazene (HACP), as a flame retardant, dispersant, and curing agent, was also designed to further improve the flame retardation performance of EP. The synergistic effect of the combination of MgAlZn-LDH-PMoA and HACP as a flame retardant and a smoke suppression agent in EP composites was investigated in detail, and the possible mechanism of reducing the fire hazard of EP composites was discussed through a variety of tests.

2. EXPERIMENTAL SECTION

2.1. Materials. Zinc nitrate hexahydrate ($Zn(NO_3)_2{\cdot}6H_2O$, ≥99.0%), aluminum nitrate nonahydrate ($Al(NO_3)_3{\cdot}9H_2O$, ≥99.0%), sodium hydroxide (NaOH), magnesium nitrate hexahydrate ($Mg(NO_3)_2{\cdot}6H_2O$, ≥99.0%), sodium carbonate (Na_2CO_3), and potassium carbonate (K_2CO_3) were supplied by Guangzhou Chemical Reagent Co., Ltd. (Guangzhou, China) and used without further purification. Phosphomolybdic acid, phosphonitrilic chloride trimer (HCCP), 4-nitrophenol, $SnCl_2$, and 4,4′-diaminodiphenylmethane (DDM) were provided by Aladdin Reagent (Shanghai) Co., Ltd. Methanol, ether, acetone, dichloromethane, and concentrated hydrochloric acid (HCl, 36.5%) were purchased from Tianjin Damao Chemical Reagent Factory (Tianjin, China). EP (E-51) was obtained from Hangzhou Wuhuigang Adhesive Co., Ltd. (China). Deionized water was produced by our institute. All chemicals used were commercially available and of analytical grade as well.

2.2. Preparation of MgAlZn-LDH-PMoA. *2.2.1. Preparation of MgAlZn-LDH-CO_3.* MgAlZn-LDH-CO_3 was synthesized by the coprecipitation method.[28] For a typical procedure, 50 mL of Na_2CO_3 (0.144 M) solution was added to a four-port flask equipped with a condensing tube, a pH meter, and two constant pressure drop funnels. Concurrently, 1.03 g of $Mg(NO_3)_2{\cdot}6H_2O$, 3.00 g of $Al(NO_3)_3{\cdot}9H_2O$, and 3.57 g of $Zn(NO_3)_2{\cdot}6H_2O$ were mixed in 150 mL of deionized water to form a homogenous solution at 50 °C and the mixed salt solution was poured into one of the funnels. Simultaneously, 50 mL of NaOH (1.0 M) solution was charged into another funnel. Coprecipitation occurred when the mixed salt solution

https://doi.org/10.1021/acsomega.2c01719
ACS Omega 2022, 7, 21714−21726

Scheme 1. Synthesis Route of the HACP Material

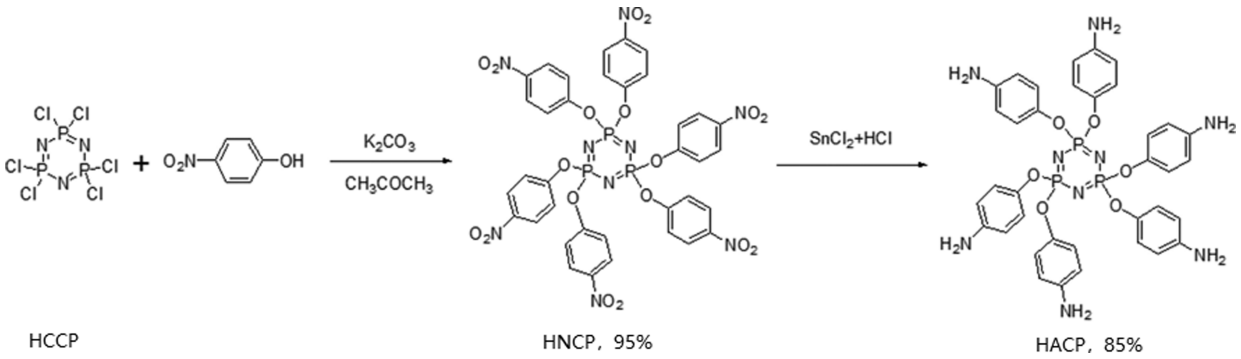

Scheme 2. Schematic Fabrication Process of EP Composites

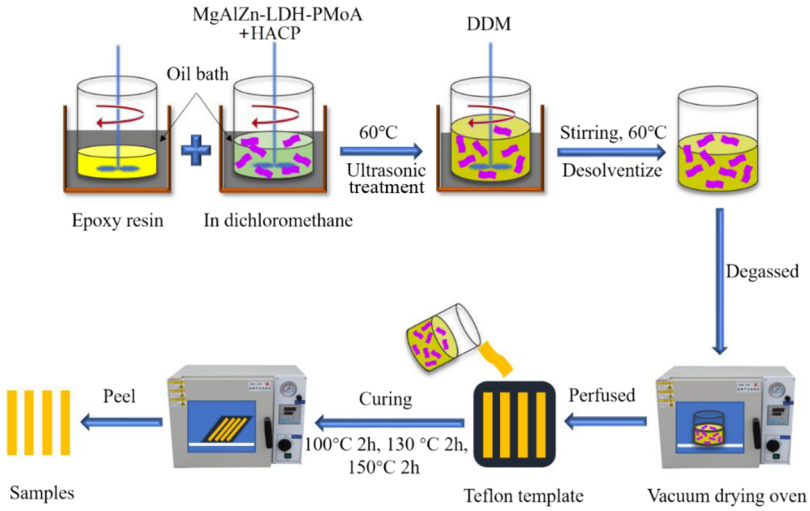

and NaOH solution were dropped into the Na_2CO_3 solution under vigorous stirring at 50 °C. Upon adjusting the dropping rate of NaOH solution, the pH of the system was controlled at 10 ± 0.2. After the salt solution was completely dripped, the reaction continued for another 24 h under vigorous stirring at 75 °C. Finally, the resulting product was filtered and washed repeatedly with deionized water until pH < 7 was achieved. The obtained product was dried in a freeze dryer for 24 h, denoted as MgAlZn-LDH-CO_3.

2.2.2. Preparation of MgAlZn-LDH-PMoA. The MgAlZn-LDH-CO_3 product was heated in a muffle furnace at 500 °C for 5 h to obtain calcinated intermediate layered dioxides (LDO). Then, 5.0 g of LDO was dispersed in 150 mL of deionized water and mechanically stirred at 70 °C for 30 min. Simultaneously, 5.0 g of phosphomolybdic acid was dissolved into 40 mL of deionized water to form a homogenous aqueous solution and added dropwise into the LDO dispersion solution under vigorous stirring at 70 °C for 2.5 h. Finally, the resulting product was filtered, thoroughly washed for 3 times, and dried in a freeze dryer for 24 h, denoted as MgAlZn-LDH-PMoA.

2.3. Synthesis of Hexakis(4-aminophenoxy)-cyclotriphosphazene (HACP). HACP was synthesized based on a previously reported method[29] as illustrated in Scheme 1, which included two preparation steps as follows:

Step 1: HCCP (10.4 g, 30 mmol) and K_2CO_3 (20.0 g, 180.2 mmol) were dissolved in dry acetone (80 mL) with effective agitation at 50 °C. Simultaneously, 4-nitrophenol (25.1 g, 0.18 mol) was first dissolved into 80 mL of acetone, the obtained solution was added dropwise to the mixture within 25 min, and the reaction mixture was stirred for 10 h under reflux. The resulting light yellow solid was filtered out, washed thoroughly with a large amount of acetone, deionized water, a little amount of methanol, and ether in order, and dried in vacuum at 55 °C for 24 h, denoted as hexa(4-nitrophenoxy)-cyclotriphosphazene (HNCP).

Step 2: Compound HNCP (7.0 g, 7.3 mmol), $SnCl_2$ (43.0 g, 190.1 mmol), and concentrated hydrochloric acid (50 mL) were mixed in ethanol (150 mL) and heated under reflux for 12 h under a nitrogen atmosphere. Then, the reaction solution was cooled to 0−2 °C overnight, and the resulting crude white solid was filtered and washed with an excess amount of acetone. Finally, the crude white solid was dissolved into deionized water to form a homogenous aqueous solution and its pH was adjusted to10 with NaOH solution; the resulting white solid (HACP) was filtered off and dried at 60 °C in vacuum for 24 h, denoted as hexa(4-aminophenoxy)-cyclotriphosphazene (HACP).

2.4. Fabrication of EP Composites. All the different EP composites were fabricated using the solution blending method. The schematic process of preparing EP composites is shown in Scheme 2. Taking the preparation of 7% MgAlZn-LDH-PMoA/HACP (2:1)/EP composite as an example, in which the total loading of the hybrid is 7 wt % and the mass ratio of MgAlZn-LDH-PMoA to HACP is 2:1, first, DDM (23.9 g) was dissolved in a small amount of dichloromethane until a uniform solution was formed. Then, MgAlZn-LDH-

https://doi.org/10.1021/acsomega.2c01719
ACS Omega 2022, 7, 21714−21726

Table 1. Components of EP Composite Samples

sample	m_1(E-51)/g	w_1(DDM)/%	w_2(MgAlZn-LDH-PMoA)/%	w_3(MgAlZn-LDH-CO_3)/%	w_4(HACP)/%
EP	100	20.0			
EP1	100	20.0		5.0	
EP2	100	20.0	5.0		
EP3	100	20.0			5.0
EP4	100	20.0	1.7		3.3
EP5	100	20.0	3.3		1.7
EP6	100	18.0	2.3		4.7
EP7	100	18.0	4.7		2.3

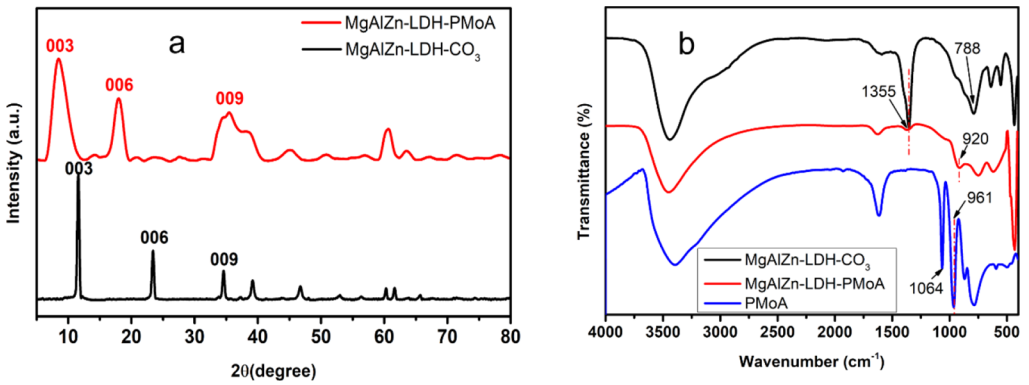

Figure 1. XRD patterns (a) and FTIR spectra (b) of MgAlZn-LDH-PMoA and MgAlZn-LDH-CO_3.

PMoA (6.0 g), HACP (3.0 g), and EP (100.0 g) were dispersed in the uniform solution, and the mixture was ultrasonically stirred for 2 h to obtain a homogeneous mixture. Subsequently, the mixture was kept in a vacuum oven at 60 °C for 2 h to remove excess dichloromethane and air.

The above mixture was poured into a polytetrafluoroethylene mold and cured at 100 °C for 2 h, 130 °C for 2 h, and 150 °C for 2 h, respectively. Finally, the obtained samples were cooled to room temperature and demoulded. The resulting sample is denoted as EP7. Similarly, pure EP, 5% MgAlZn-LDH-PMoA/HACP (1:2)/EP, 5% MgAlZn-LDH-PMoA/HACP (2:1)/EP, and 7% MgAlZn-LDH-PMoA/HACP (1:2) were prepared subsequently and were named EP, EP4, EP5, and EP6, respectively. For comparison, 5% MgAlZn-LDH-CO_3/EP, 5% MgAlZn-LDH-PMoA/EP, and 5% HACP/EP were also prepared using the same procedure and were named EP1, EP2, and EP3, respectively. The components of EP composites are listed in Table 1.

2.5. Characterization. X-ray diffraction (XRD) measurements were carried out using a Malvern Panalytical Aeris (Netherlands) at room temperature with a scan rate of 5°/min from 5 to 80° and equipped with a CuKα tube and an Ni filter (λ = 0.1542 nm).

Fourier transform infrared (FTIR) spectroscopy was performed with a Nicolet 6700 FTIR spectrophotometer (Thermo Fisher Scientific, USA), and the sample pellets containing KBr powder were analyzed in the range of 4000−400 cm^{-1}.

The ^{1}H nuclear magnetic resonance (NMR) and ^{31}P NMR spectra were recorded using an Avance III 400 MHz NMR spectrometer (Bruker, Switzerland) using deuterated dimethyl sulfoxide (DMSO-d_6) as a solvent at room temperature.

Scanning electron microscopy (SEM) images of the char residue structure were obtained using a Hitachi SU8220 instrument (Japan).

The thermogravimetric analysis (TGA) was performed using a TGA/DSC3+ instrument (Mettler Toledo, Switzerland). The thermal stabilities of the flame retardants, pure EP, and EP composites were determined at a heating rating of 10 °C/min under a nitrogen atmosphere.

The cone calorimeter combustion tests were performed using a cone calorimeter (Fire Testing Technology, UK) according to the procedures specified in the ISO5660 standard with a heat radiation of 35 kW/m^2, and the size of all the samples was 100 × 100 × 3 mm^3.

According to the standard ASTM D2863, the limiting oxygen index (LOI) values were measured using an HC-2 oxygen index instrument (Jiangning Analytical Instruments, China), and the sizes of all the specimens were 100 × 10 × 3 mm^3.

According to the standard ASTM D3801, the UL94 vertical burning test was carried out on a PX-03-001 instrument (Suzhou Phoenix Instruments Co., Ltd., China) with a sample size of 125 × 13 × 3 mm^3, and the combustion process of all samples was recorded by a digital camera.

Smoke density tests were recorded on a JSC-2 smoke density test instrument (made in China) according to the standard ISO 5659-2 with a heat radiation of 25 kW/m^2. The dimension of all the specimens was 75 × 75 × 3 mm^3.

Laser Raman spectroscopy was carried out with a SPEX-1403 laser Raman spectrometer (SPEX Co., USA) at room temperature using the back scattered geometry of 514.5 nm argon laser line.

3. RESULTS AND DISCUSSION

3.1. Characterization of MgAlZn-LDH-PMoA. The XRD patterns of MgAlZn-LDH-CO_3 and MgAlZn-LDH-PMoA are shown in Figure 1a. In the XRD pattern of MgAlZn-LDH-CO_3, the characteristic diffraction peaks at 11.68, 23.52, and

https://doi.org/10.1021/acsomega.2c01719
ACS Omega 2022, 7, 21714−21726

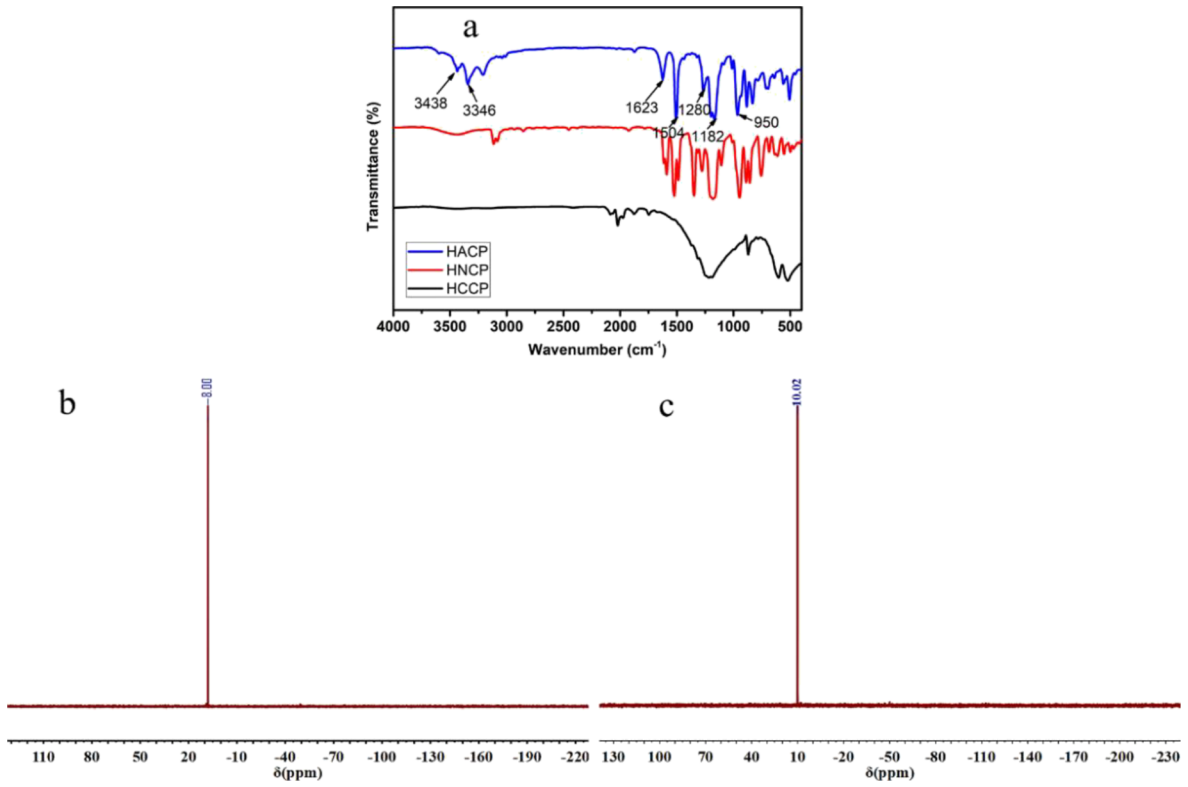

Figure 2. FTIR spectra (a) and ^{31}P NMR (b, c) spectra of HNCP and HACP.

34.73° can be attributed to the (003), (006), and (009) diffraction peaks, respectively.[30]

After calcination and reconstruction, all the diffraction peaks can be detected in the XRD pattern of MgAlZn-LDH-PMoA, indicating that the ordered layered crystal structure is reconstructed. In addition, the characteristic peaks of (003) and (006) for MgAlZn-LDH-PMoA are shifted to low angles at 8.37 and 17.56°, respectively. Therefore, the corresponding layer spacing of LDHs enlarged from 0.76 and 0.38 nm to 1.06 and 0.49 nm, respectively. The interlayer spacing in MgAlZn-LDH-PMoA is almost the same as the diameter of the short axis of PMoA, which is almost consistent with a previously reported study.[31] The results primarily revealed that the anion $[PMo_{12}O_{40}]^{3-}$has been intercalated into the LDH interlayers efficiently.

Figure 1b shows the FTIR spectra of PMoA, MgAlZn-LDH-CO_3, and MgAlZn-LDH-PMoA. In the FTIR spectrum of PMoA, an obvious absorption peak at 961 cm^{-1} is due to the stretching vibration of Mo−O, while the peak at 1064 cm^{-1} corresponds to the vibration of the P−O bond. In the MgAlZn-LDH-CO_3 spectrum, an intense broad band at 3450 cm^{-1} is assigned to the O−H group in the LDH layers. The lattice vibration of Mg−O, Al−O, and Zn−O groups can be observed in the low frequency region below 800 cm^{-1}.[31] Also, the strong absorption bands near 1355 and 788 cm^{-1} could be designated as the vibrational absorption bands of CO_3^{2-}(v_3) and CO_3^{2-} (v_2).[32] Compared with MgAlZn-LDH-CO_3, the FTIR spectrum of MgAlZn-LDH-PMoA shows very little absorption near 1355 cm^{-1}, indicating that there is almost no CO_3^{2-} in the interlayer of MgAlZn-LDH-PMoA. Also, the characteristic absorption bands for the Mo−O bond shifted to a lower frequency at 920 cm^{-1} in MgAlZn-LDH-PMoA, which is mainly due to the electrostatic interaction between the host layers and the guest anions.[33]

3.2. Characterization of HACP. The FTIR spectrum of HACP is shown in Figure 2a. The characterized absorption peaks, which were observed at 3438 and 3346 cm^{-1} (−NH_2), 3048 cm^{-1} (C−H), 1623 cm^{-1} (C−C), 1504 cm^{-1} (benzene ring), 1182 cm^{-1} (P═N), 1280 cm^{-1} (P−N), and 950 cm^{-1} (P−O−C), indicated the successful synthesis of HACP.[34] To ensure the purity of HNCP and HACP, ^{31}P NMR measurements were carried out, and the results are shown in Figure 2b,c. In the ^{31}P NMR spectra of HNCP and HACP, there are no characteristic peaks except those at 8.00 and 10.02 ppm, respectively. In conclusion, all the results confirmed the successful synthesis of HACP.

3.3. Thermogravimetric Properties of MgAlZn-LDH-PMoA and HACP. Figure 3 shows the TGA curves of MgAlZn-LDH-CO_3, MgAlZn-LDH-PMoA, and HACP under

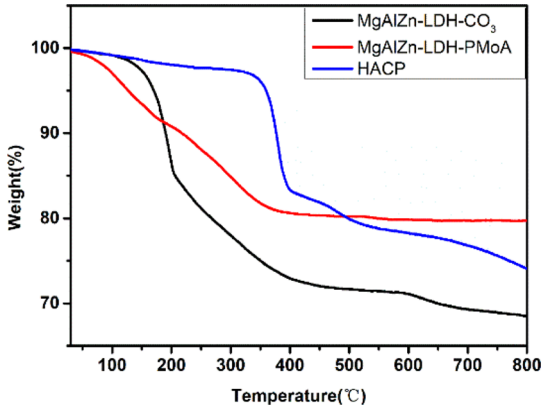

Figure 3. TGA curves of MgAlZn-LDH-CO_3, MgAlZn-LDH-PMoA, and HACP materials.

https://doi.org/10.1021/acsomega.2c01719
ACS Omega 2022, 7, 21714−21726

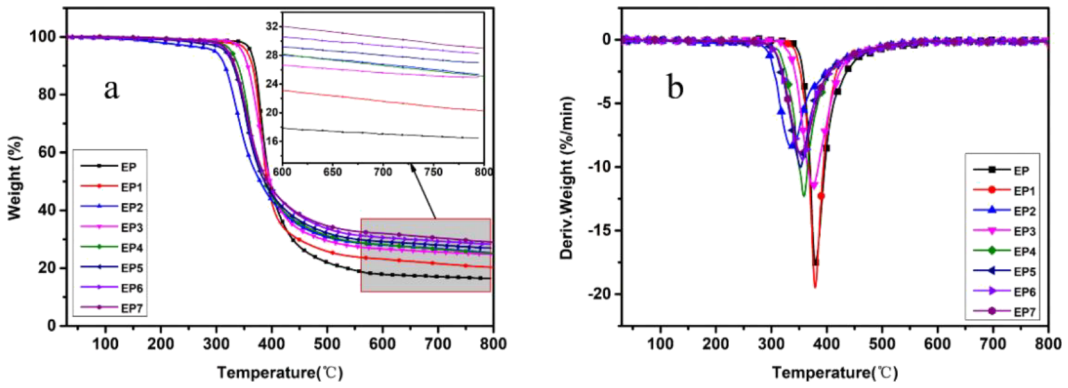

Figure 4. TGA (a) and DTG (b) profiles of neat EP and its composites under a nitrogen atmosphere.

nitrogen conditions. For LDHs, the evaporation of surface-adsorbed water and the elimination of interlayer crystallization water mainly occur when the temperature is below 200 °C. When the temperature is raised from 200 to 400 °C, the weight loss is caused by dehydroxylation and deionization of LDHs. With the increase of temperature, hydrotalcite can completely become a dense metal oxide.[35,36] It can be observed that MgAlZn-LDH-CO_3 and MgAlZn-LDH-PMoA show an obvious weight loss of adsorbed water and crystallization water below 200 °C. The weight loss for MgAlZn-LDH-CO_3 observed between 200 and 400 °C is mainly caused by dehydroxylation and deionization of CO_3^{2-}. As for MgAlZn-LDH-PMoA, the TGA curve is different from that of MgAlZn-LDH-CO_3 because the thermal stability of metal polyoxometalate $PMo_{12}O_{40}^{3-}$ is better than that of volatile anion CO_3^{2-}, which indirectly proves that $PMo_{12}O_{40}^{3-}$ has successfully replaced CO_3^{2-}. In addition, it is observed from the TGA curves that the residue of MgAlZn-LDH-PMoA at 800 °C is 79.8%, which is significantly higher than that of MgAlZn-LDH-CO_3 (68.5%). The excellent thermal stability of MgAlZn-LDH-PMoA is of great significance to reduce the fire risk of polymers.

As for the TGA curves of HACP, the weight loss at 350 °C is only 3.9%, indicating that the compound has good thermal stability. In addition, 74 wt % of the residue remained after HACP was pyrolyzed at 800 °C, which shows that HACP would be a good candidate for flame retardant components as an excellent carbonization agent.

3.4. Thermal Stability of EP Composites. The thermal stability of pure EP and EP composites was studied by TGA. The TGA and derivative thermogravimetry (DTG) curves of pure EP and EP composites in a nitrogen atmosphere are shown in Figure 4, and the specific values from the TGA and DTG curves are listed in Table 2. Specifically, the initial decomposition temperature ($T_{5\%}$), the maximum degradation rate of degradation temperature (T_{max}), and the char yield are all important parameters to evaluate the thermal stability of EP composites.

Table 2. Thermal Properties of Neat EP and Its Composites under a Nitrogen Atmosphere

sample	$T_{5\%}$ (°C)	T_{max} (°C)	residue at 800 °C (wt %)
EP	362.0	379.4	16.5
EP1	355.1	378.9	20.3
EP2	297.4	335.3	25.3
EP3	346.4	374.6	24.9
EP4	326.9	357.9	25.1
EP5	316.1	352.9	27.0
EP6	320.2	356.2	28.3
EP7	321.2	351.4	29.0

From Figure 4a,b, it is obvious that the temperature of $T_{5\%}$ and T_{max} of the pure EP matrix is 362.0 and 379.4 °C, respectively. However, $T_{5\%}$ and T_{max} of all the EP composites decreased in varying degrees compared with EP; this is mainly caused by the metal oxides and phosphoric acid compounds formed from LDHs and HACP to promote the pyrolysis and carbonization of the EP matrix at a lower temperature. The early initial decomposition is a necessary process for lowering the temperature of the polymer matrix and forming a char layer. Obviously, the thermal degradation of pure EP in the range of 350−600 °C shows only one stage and corresponds to the DTG pattern, which is corresponding to the decomposition of three-dimensional macromolecular chains of the polymer. All the EP composites exhibited a one-step degradation behavior similar to pure EP.

It is observed that the char residue of the pure EP matrix is only 16.5% at 800 °C. With a loading of 5 wt % of MgAlZn-LDH-CO_3, MgAlZn-LDH-PMoA, and HACP into the EP matrix, the char residue of EP composites at 800 °C increased to 20.3, 25.3, and 24.9%, respectively, which indicated that these three compounds can promote the carbonization of EP effectively. As expected, the incorporation of MgAlZn-LDH-PMoA and HACP showed a synergistic effect on promoting char formation of EP composites (such as EP5) compared with the EP matrix filled with only MgAlZn-LDH-PMoA or HACP. Particularly, the char yield of EP7 was as high as 29.0%, indicating that hybrids had a synergistic effect on promoting char formation. The formed compact residual char during pyrolysis can adhere to the polymer surface and reduce heat transfer and the entry of oxygen, thus reducing the release of flue gases.

3.5. Combustion Behavior. *3.5.1. Cone Calorimeter.* The flammability behavior of pure EP and EP composites was investigated by means of a cone calorimeter, which is considered as an effective method to simulate real fire disasters. The HRR and THR of EP and EP composites are shown in Figure 5. Also, some important corresponding parameters obtained from the cone calorimeter tests are summarized in Table 3.

It is clear that the pure EP is highly flammable whose PHRR and THR values reach 1133.2 $kW \cdot m^{-2}$ and 96.9 $MJ \cdot m^{-2}$, respectively. However, the PHRR and THR values of EP2 are reduced by 43.3 and 13.6%, respectively, compared with the

https://doi.org/10.1021/acsomega.2c01719
ACS Omega 2022, 7, 21714−21726

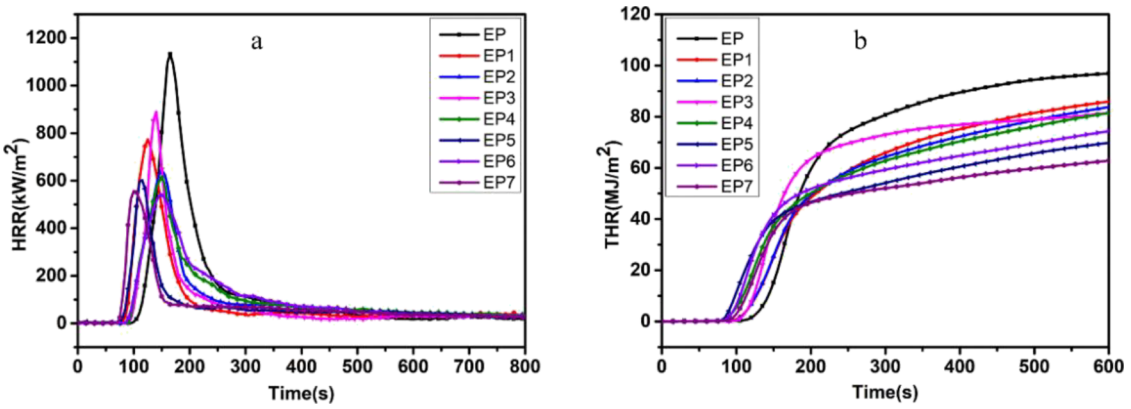

Figure 5. Heat release rate (HRR) (a) and THR (b) versus time curves of neat EP and its composites with a combustion calorimeter.

Table 3. Cone Calorimeter Data of EP and Its Composites

sample	THR (MJ m^{-2})	PHRR (kW m^{-2})	TSP (m^2)	COP (g/s)	CO_2P (g/s)
EP	96.9	1133.2	23.0	0.03556	0.5483
EP1	85.9	773.5	17.6	0.02093	0.3902
EP2	83.7	642.8	17.3	0.01823	0.2875
EP3	81.5	889.8	21.8	0.04104	0.4506
EP4	81.4	612.7	17.2	0.02723	0.4164
EP5	69.8	601.9	13.2	0.01862	0.2693
EP6	74.4	539.1	14.9	0.02530	0.4197
EP7	62.8	556.5	12.9	0.01806	0.2686

pure EP, which is more obvious than EP1. This is mainly due to the physical barrier effect[37,38] in the solid of metal oxides formed by MgAlZn-LDH-PMoA at a high temperature. Also, further inhibition of the volatilization of combustible gas and the transmission of oxygen during the decomposition process of the composite occurred.[39,40] Moreover, compared with EP, the PHRR and THR values of EP3 decreased by 21.5 and 15.9%, respectively, which indicated that when only HACP is used as the flame retardant (FR), the flammability behavior is not effective. In particular, it should be noted that the PHRR and THR values of EP5 decreased by 46.9 and 28.0%, respectively, which are more than the values of EP2 and EP3. This indicates the synergistic effect of MgAlZn-LDH-PMoA and HACP. When we increased the amount of the FRs as 7% in EP6 and EP7, the PHRR and THR values decreased effectively with the more loading of FRs. Upon addition of both MgAlZn-LDH-PMoA and HACP, the flame retardant elements in the condensed phase improve the compactness of the residual char. Moreover, MgAlZn-LDH-PMoA can absorb part of the heat of the flame zone and release water vapor in the process of combustion, which plays the role of dilution and cooling, and achieves a better effect of reducing fire hazard.

3.5.2. LOI and Vertical Burning Test (UL-94). The LOI and UL-94 burning tests are two important parameters to further estimate the combustion and flammability performance of polymer materials. As shown in Figure 6a, the LOI value of pure EP is 25.0%, which indicates that it is combustible in air. However, the LOI values of EP composites all increased at different levels after loading different fractions of flame retardants into the EP matrix. The LOI value of EP composites increased greatly while MgAlZn-LDH-PMoA and HACP were added together into the EP matrix. Moreover, the LOI value of the EP composite containing 7 wt % MgAlZn-LDH-PMoA and HACP increased to 30.5 and 31.0%, respectively. In the vertical burning test (UL-94) shown in Figure 6b, the fire of pure EP spreads rapidly and is accompanied by the production of molten drippings without significant self-extinguishing phenomenon after ignition. In contrast, EP composites containing different flame retardants do not produce molten droplets during combustion and can be self-extinguished (Figure S1). EP7 exhibited the most obvious flame retardant property, which can extinguish itself only 35 s after ignition, and the amount of smoke produced during combustion is the least. Obviously, the incorporation of MgAlZn-LDH-PMoA and HACP can improve the flame retardant properties of EP composites.

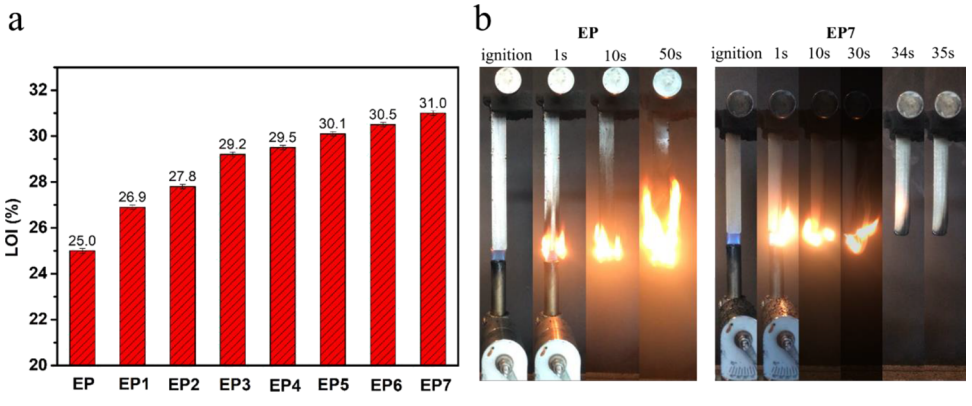

Figure 6. LOI values of the neat EP and EP composites (a) and the vertical burning test result of EP and EP7 (b).

https://doi.org/10.1021/acsomega.2c01719
ACS Omega 2022, 7, 21714−21726

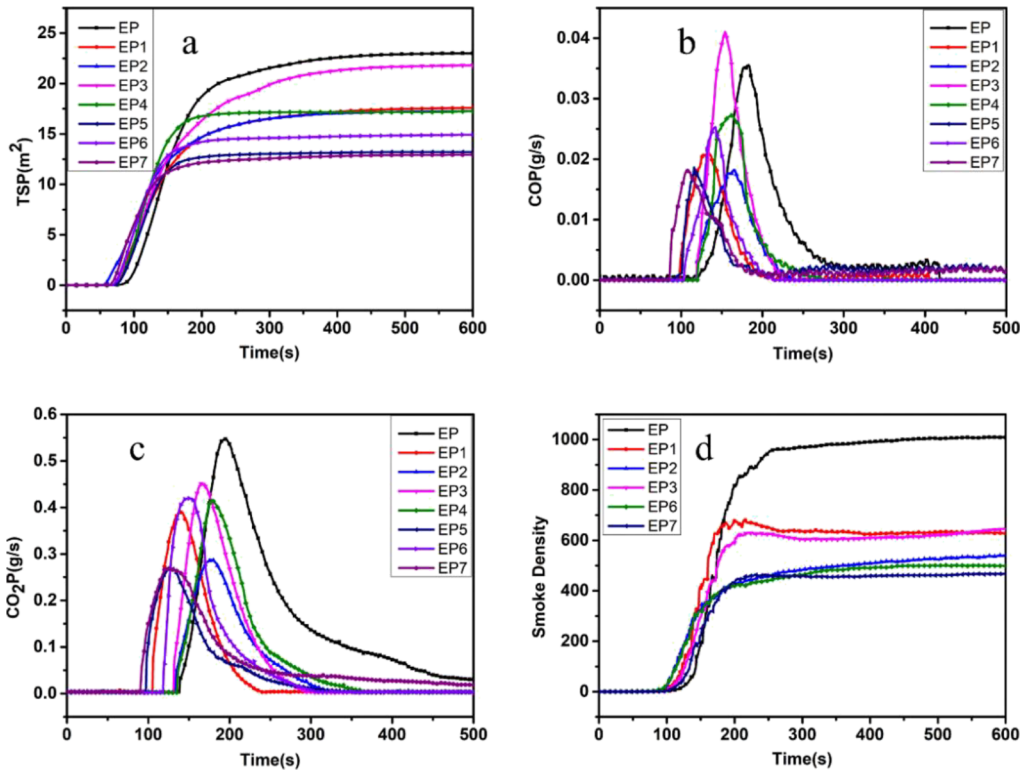

Figure 7. Total Smoke Production (TSP) (a), CO (b), CO_2 (c), and smoke density (d) yield versus time curves of neat EP and its composites with a combustion calorimeter.

3.6. Smoke Toxicity of EP and Its Composites. Smoke toxicity is another important parameter to evaluate the fire risk of polymers because thermal radiation is released by toxic CO and primary CO_2 oxidation gases during polymer combustion.[41] Therefore, reducing the amount of smoke, CO, and primary CO_2 produced in the process of polymer combustion is of great significance to reduce the fire risk. Figure 7 shows the TSP, CO, CO_2, and smoke density yield curves of EP and EP composites tested by a cone calorimeter, and the specific data are shown in Table 3.

It can be seen from Figure 7 that upon the incorporation of MgAlZn-LDH-PMoA and HACP hybrids into the EP matrix, the emission of smoke and combustible gas could be significantly reduced. As shown in Table 3, the production of TSP, maximum CO, and CO_2 yields of pure EP is as high as 23.0 m^2, 0.03556 g/s, and 0.5483 g/s, respectively. It should be noted that the TSP and maximum CO values of the samples containing MgAlZn-LDH-PMoA are relatively low, and the release of CO has been reduced by 48.7% compared with pure EP, which shows that MgAlZn-LDH-PMoA can reduce the smoke toxicity of flammable gases. The main reason is that MgAlZn-LDH-PMoA promotes the carbonization of EP through catalysis, thus reducing the release of oxides in the gas phase.[42,43] Meanwhile, it was obviously seen that the addition of MgAlZn-LDH-PMoA and HACP hybrids had a great influence on reducing TSP, CO, and CO_2 production during the combustion process, and the reduction effect of EP5 and EP7 is the most obvious compared with other composites, which is due to the outstanding synergistic effect between MgAlZn-LDH-PMoA and HACP.

The synergistic effect of MgAlZn-LDH-PMoA and HACP on smoke suppression of EP was further studied by the smoke density test. The smoke density curves of pure EP and EP composites are shown in Figure 7d. Notably, the maximum smoke density (Ds, max) of pure EP is 1008.42. The smoke density of EP composites decreased with the addition of different flame retardants, reaching 37.79, 46.39, 36.05, 50.54, and 53.68%, respectively. Among them, the smoke density of EP7 with MgAlZn-LDH-PMoA and HACP is obviously lower than that of EP composites with a single component. The main reason is that MoO_3 formed by PMoA degradation and the phosphoric acid compounds formed by HACP at high temperatures simultaneously promote the catalytic carbonization of the EP matrix, thus reducing the emission of smoke.[40]

3.7. Flame Retardancy Mechanism. *3.7.1. Gaseous Phase.* In general, the thermal degradation of the polymer matrix is accompanied by the release of gaseous volatiles under an anaerobic atmosphere.[13] Therefore, TG−IR coupling technology is widely used in the evaluation and determination of volatile compounds in the thermal degradation of polymers. The intensities of the samples and evolved gaseous products versus time of pure EP and EP7 composite are shown in Figures 8 and S2; the strongest signals of the characteristic gaseous products of pure EP and EP7 composite are similar, indicating that the addition of MgAlZn-LDH-PMoA and HACP did not change the types of decomposition products. Several characteristic peaks for the primary pyrolysis products of pure EP and EP7 are listed as follows: 2190 cm^{-1} (CO), 2360 cm^{-1} (CO_2), 2930 cm^{-1} (hydrocarbons), 1740 cm^{-1} (carbonyl compounds), and 1510 cm^{-1} (aromatic compounds).[44] The experiment was also carried out by using EP/HACP (EP3) as a comparison and found that the total toxic volatile intensity of EP3 composites is lower than that of pure EP during the combustion process (Figure S3). Particularly, with the addition of MgAlZn-LDH-PMoA and

https://doi.org/10.1021/acsomega.2c01719
ACS Omega 2022, 7, 21714−21726

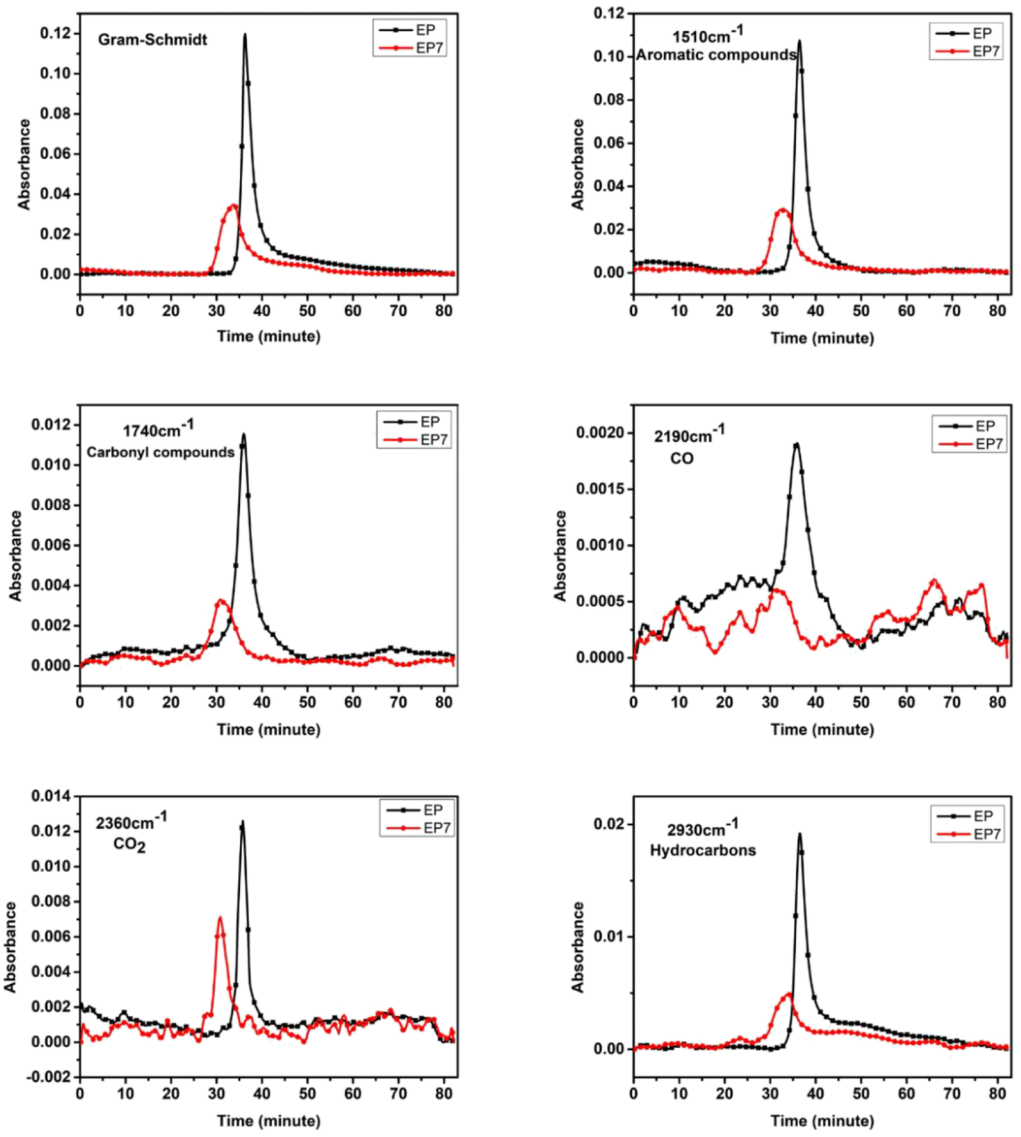

Figure 8. Absorbance of pyrolysis products for neat EP and its composite EP7 versus time.

HACP, the maximum absorbance intensities of all typical pyrolysis gas products dramatically decreased compared to pure EP, indicating that the synergistic effect between the two flame retardants can inhibit the release of gas products. Among them, the reduction of the concentration of flammable pyrolysis products and toxic substances can enhance the safety against fire.

3.7.2. Condensed Phase. To further clarify the responsible mechanism of flame retardancy, the char residues of pure EP and EP composites after the cone calorimeter test were directly observed through digital photos as shown in Figure 9a,b. The morphology and microstructure of char residues of EP and its composites are presented in Figure 9c.

Compared with pure EP, when the hydrotalcite MgAlZn-LDH-PMoA is introduced into the EP, the sample EP2 will form a complete carbon layer structure after combustion, and the thickness of the carbon layer increases significantly. The white substances on the surface of the carbon layer are mainly metal oxides formed after the combustion of hydrotalcite. It can be seen from Figure 9 EP2(c) that the structure of these carbon layers is very dense. These dense carbon layer structures cover the surface of the polymer matrix, helping to reduce heat release and the generation of toxic fumes. From Figure 9 EP(a,b) and EP3(a,b), it can be seen that pure EP only generates a little carbon residual after combustion and exposes the white aluminum foil, while the EP3 composite generates a large amount of black carbon residual after combustion. The thickness of the carbon layer is improved compared to pure EP. From their SEM images, Figure 9 EP(c) and EP3(c), it can be seen that many cracks and holes appear on the surface of pure EP after combustion, and no dense carbon layer is formed. However, after the combustion of EP3 composites, the surface carbon layer shows an increase in density without many cracks and holes. The reason may be that the flame retardant HACP will decompose during the combustion process to generate phosphorus-containing compounds to promote the carbon residue generated in the EP matrix, thereby improving the flame retardant properties of the composites.

It is known that the compactness and degree of graphitization of the carbon residue play an important role in suppressing the exothermic and pyrolytic volatilization of the internal matrix. The carbon residue morphology and microstructure of pure EP and EP7 composites are shown in

https://doi.org/10.1021/acsomega.2c01719
ACS Omega 2022, 7, 21714−21726

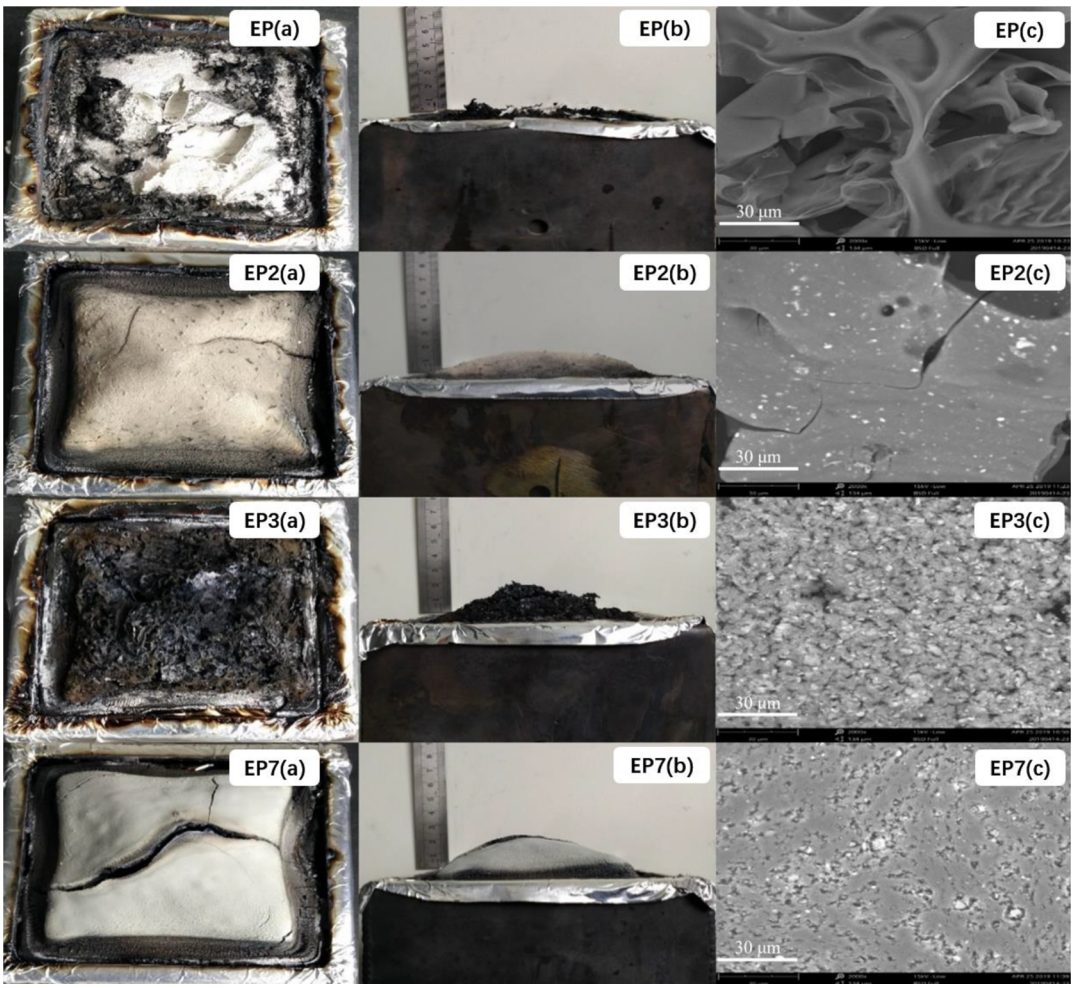

Figure 9. Digital photographs (a, b) and SEM images (c) of burning residues (EP, EP2, EP3, and EP7) obtained after cone calorimetry.

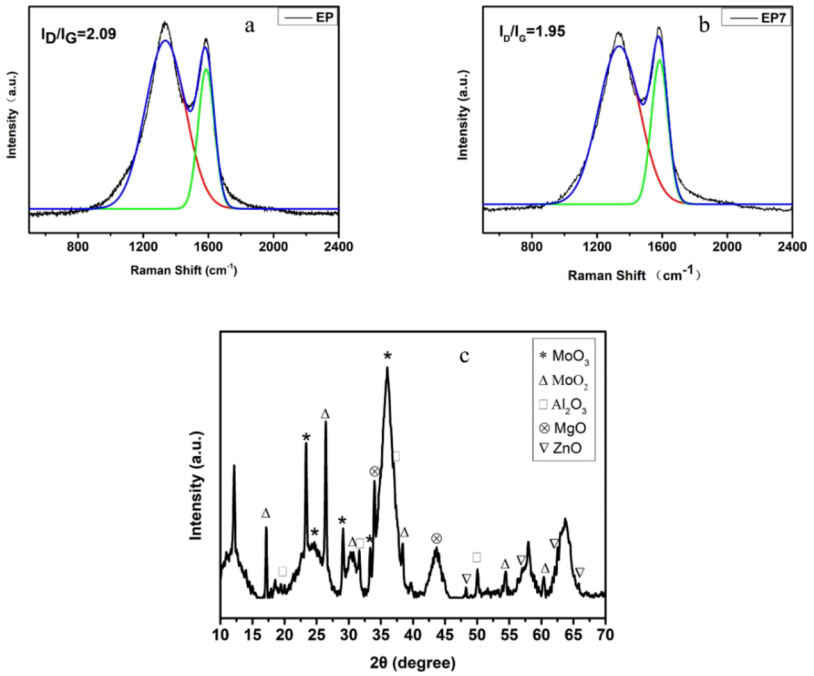

Figure 10. Raman spectra of the neat EP (a) and EP7 (b) and XRD patterns of the char residue of EP7 (c).

https://doi.org/10.1021/acsomega.2c01719
ACS Omega 2022, 7, 21714−21726

Scheme 3. Abridged General View of the Flame Retardancy Mechanism for the Effect of MgAlZn-LDH-PMoA and HACP on EP

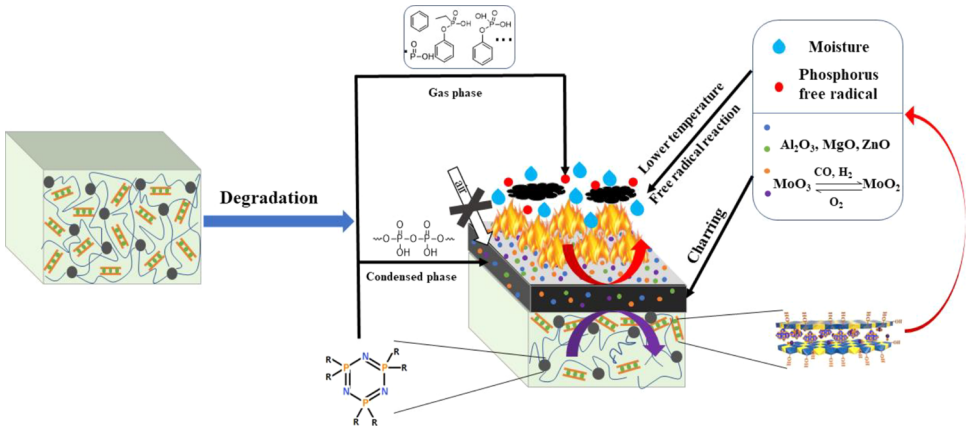

Figure 9 EP and EP7. Through SEM observation, after adding both flame retardants HACP and MgAlZn-LDH-PMoA, the surface carbon layer of EP7 composites is dense and relatively complete, which can delay heat and mass transfer and effectively prevent further combustion of the internal polymer matrix.

In Figure 9, by comparing EP, EP2, and EP3, we can see that after the addition of either MgAlZn-LDH-PMoA(EP2) or HACP(EP3) into EP, there are some holes and cracks in the surface, but the char residues of EP composites were relatively integrated. Meanwhile, by comparing EP, EP2, EP3, and EP7, we can see that the char residue of EP7 is more compact than any other samples, which means that the coexistence of FRs is better than the presence of a single component or pure EP without FRs as observed after combustion by visual observation.

As an important characterization method to study the compactness and graphitization degree of residual chars, EP and EP7 were investigated by Raman spectroscopy after being tested by a cone calorimeter. As shown in Figure 10a,b, there are two strong absorption peaks about 1345 and 1585 cm^{-1}, respectively, which are the representative peaks of graphite (D and G peaks). In general, the graphitization state of residual carbon is calculated by using the ratio of D band to G band integral strength (I_D/I_G). The lower the I_D/I_G value, the higher the graphitization degree of residual chars. Typically, the higher the carbon content of graphite, the denser the carbon layer, and the more obvious the effect of preventing heat diffusion and material degradation.[45] Obviously, the I_D/I_G value of pure EP was 2.09, while the I_D/I_G value of the EP7 composite was only 1.95. The results show that MgAlZn-LDH-PMoA and HACP can promote the formation of graphitized carbon, so as to improve its flame retardant and smoke suppression properties.

The coke residue of EP7 was further analyzed by XRD. The characteristic peaks of MoO_3, MoO_2, Al_2O_3, MgO, and ZnO are shown in Figure 10c. Among them, MoO_3 would be reduced to MoO_2 by many reducing gases (CO and H_2) produced by epoxy polymers during the decomposition. At the same time, MoO_2 would also be oxidized to MoO_3 at a high temperature. This redox cycle process will greatly reduce the toxic and harmful gases generated during the EP combustion process. This result also confirms that MgAlZn-LDH-PMoA can generate MoO_3 during the combustion process. In addition, MgAlZn-LDH-PMoA can also catalyze the carbonization of degradation products, which will become an important part of the barrier and further reduces the heat transfer.

Based on the analysis of the gas−solid phase, we proposed a possible flame retardancy and smoke suppression mechanism of the synergistic effect of MgAlZn-LDH-PMoA and HACP on EP, which is shown in Scheme 3. When the temperature is lower than 200 °C, LDHs can absorb heat by dehydration to achieve the flame retardant effect. At high temperatures, HACP can not only pyrolyze into phosphorus-containing gaseous products and free radicals, which could capture other free radicals generated by EP decomposition during the combustion process, but also the resulting phosphorus compounds can improve the adhesion and strength of the char generated by the EP substrate. Meanwhile, the char captured a large amount of metal oxides (MoO_3, MoO_2, Al_2O_3, MgO, and ZnO) produced by the pyrolysis of MgAlZn-LDH-PMoA, which further enhances its strength. It is worth noting that the formation of MoO_3 can not only reduce the combustible gas released by the gas-phase redox reaction but also increase the density of the condensed phase to prevent heat transfer. Accordingly, the gas phase and condensed phase of EP/MgAlZn-LDH-PMoA act simultaneously in the combustion process, which makes EP to have excellent flame retardant and smoke suppression properties.

4. CONCLUSIONS

$PMo_{12}O_{40}^{3-}$ was successfully intercalated into the interlayer space of LDHs by the coprecipitation reconstruction method. Finally, the inorganic flame retardant MgAlZn-LDH-PMoA containing various flame retardant elements was obtained. In addition, HACP, as a flame retardant, curing agent, and dispersant, is used in the flame retardant of EP together with MgAlZn-LDH-PMoA, which has a significant synergistic flame retardant effect with MgAlZn-LDH-PMoA based on LOI and UL-94 tests. Notably, the addition of 5 wt % of composite flame retardant can make the LOI value reach the flame retardant standard of polymer materials. Meanwhile, the cone calorimeter test results show that the PHRR of EP7 decreased by 50.9%. The main reason for the decline of the fire resistance of the composite is the physical barrier of the flame retardant and catalytic carbonization. Furthermore, a variety of metal oxides formed in the combustion process of MgAlZn-LDH-PMoA can promote the formation of a denser char layer, which

https://doi.org/10.1021/acsomega.2c01719
ACS Omega 2022, 7, 21714−21726

can not only inhibit the transfer of volatile combustion gas and heat but also achieve a good flame retardant and smoke suppression effect. Meanwhile, MoO_3 decomposed from $PMo_{12}O_{40}^{3-}$ not only promotes char layer formation during combustion but also reduces the emission of toxic gases such as CO through a redox reaction, thus further improving the fire safety performance.

■ ASSOCIATED CONTENT

Supporting Information

The Supporting Information is available free of charge at https://pubs.acs.org/doi/10.1021/acsomega.2c01719.

Digital photos of EP and EP composites during the UL-94 vertical burning test process (Figure S1); three-dimensional variation spectra of pyrolysis products for EP and EP7 (Figure S2); and absorbance of pyrolysis products for EP and EP/HACP composites versus time (Figure S3) (PDF)

■ AUTHOR INFORMATION

Corresponding Authors

Zhifeng Hao − *Key Laboratory of Clean Chemistry Technology of Guangdong Regular Higher Education Institutions, School of Chemical Engineering and Light Industry, Guangdong University of Technology, Guangzhou 510006, P. R. China;* orcid.org/0000-0002-9731-1504; Email: haozf@gdut.edu.cn

Yingmin Huang − *Guangzhou Panyu Cable Group Co., Ltd, Guangzhou 510006, P. R. China*; Email: standfist@163.com

Authors

Xiang Chen − *Key Laboratory of Clean Chemistry Technology of Guangdong Regular Higher Education Institutions, School of Chemical Engineering and Light Industry, Guangdong University of Technology, Guangzhou 510006, P. R. China;* orcid.org/0000-0002-3016-620X

Bingyi Wang − *Key Laboratory of Clean Chemistry Technology of Guangdong Regular Higher Education Institutions, School of Chemical Engineering and Light Industry, Guangdong University of Technology, Guangzhou 510006, P. R. China*

Guizhen Tan − *Key Laboratory of Clean Chemistry Technology of Guangdong Regular Higher Education Institutions, School of Chemical Engineering and Light Industry, Guangdong University of Technology, Guangzhou 510006, P. R. China*

Mohamed S. Selim − *Key Laboratory of Clean Chemistry Technology of Guangdong Regular Higher Education Institutions, School of Chemical Engineering and Light Industry, Guangdong University of Technology, Guangzhou 510006, P. R. China; Petroleum Application Department, Egyptian Petroleum Research Institute, 11727 Cairo, Egypt*

Jian Yu − *Key Laboratory of Clean Chemistry Technology of Guangdong Regular Higher Education Institutions, School of Chemical Engineering and Light Industry, Guangdong University of Technology, Guangzhou 510006, P. R. China*

Complete contact information is available at: https://pubs.acs.org/10.1021/acsomega.2c01719

Author Contributions

‖X.C. and B.W. contributed equally to this work.

Notes

The authors declare no competing financial interest.

■ ACKNOWLEDGMENTS

This work was supported by the Applied Science and Technology Research and Development Special Foundation of Guangdong Province (Grant No.: 2016B090930004) and the National Natural Science Foundation of China (Grant No. 52150410401).

■ REFERENCES

(1) Kalali, E. N.; Wang, X.; Wang, D. Y. Multifunctional intercalation in layered double hydroxide: toward multifunctional nanohybrids for epoxy resin. *J. Mater. Chem. A* **2016**, *4*, 2147−2157.

(2) Jian, R. K.; Ai, Y. F.; Xia, L.; Zhao, L. J.; Zhao, H. B. Single component phosphamide-based intumescent flame retardant with potential reactivity towards low flammability and smoke epoxy resins. *J. Hazard. Mater.* **2019**, *371*, 529−539.

(3) Jian, R. K.; Wang, P.; Duan, W. S.; Wang, J. S.; Zheng, X. L.; Weng, J. B. Synthesis of a novel P/N/S-containing flame retardant and its application in epoxy resin: thermal property, flame retardance, and pyrolysis behavior. *Ind. Eng. Chem. Res.* **2016**, *55*, 11520−11527.

(4) Zhang, Z. Y.; Yuan, L.; Liang, G. Z.; Gu, A. J.; Qiang, Z. X.; Yang, C. W.; Chen, X. X. Unique hybridized carbon nanotubes and their high performance flame retarding composites with high smoke suppression, good toughness and low curing temperature. *J. Mater. Chem. A* **2014**, *2*, 4975−4988.

(5) Ma, C.; Qiu, S. L.; Yu, B.; Wang, J. L.; Wang, C. M.; Zeng, W. R.; Hu, Y. Economical and environment-friendly synthesis of a novel hyperbranched poly (aminomethylphosphine oxide-amine) as co-curing agent for simultaneous improvement of fire safety, glass transition temperature and toughness of epoxy resins. *Chem. Eng. J.* **2017**, *322*, 618−631.

(6) Jiang, Y.; Hao, Z. F.; Luo, H. S.; Shao, Z. H.; Yu, Q.; Sun, M.; Ke, Y.; Chen, Y. L. Synergistic effects of boron-doped silicone resin and a layered double hydroxide modified with sodium dodecyl benzenesulfonate for enhancing the flame retardancy of polycarbonate. *RSC Adv.* **2018**, *8*, 11078−11086.

(7) Wang, D. Y.; Leuteritz, A.; Wang, Y. Z.; Wagenknecht, U.; Heinrich, G. Preparation and burning behaviors of flame retarding biodegradable poly (lactic acid) nanocomposite based on zinc aluminum layered double hydroxide. *Polym. Degrad. Stab.* **2010**, *95*, 2474−2480.

(8) Edenharter, A.; Feicht, P.; Diar-Bakerly, B.; Beyer, G.; Breu, J. Superior flame retardant by combining high aspect ratio layered double hydroxide and graphene oxide. *Polymer* **2016**, *91*, 41−49.

(9) Nyambo, C.; Songtipya, P.; Manias, E.; Jimenez-Gasco, M. M.; Wilkie, C. A. Effect of MgAl-layered double hydroxide exchanged with linear alkyl carboxylates on fire-retardancy of PMMA and PS. *J. Mater. Chem.* **2008**, *18*, 4827−4838.

(10) Nyambo, C.; Chen, D.; Su, S. P.; Wilkie, C. A. Does organic modification of layered double hydroxides improve the fire performance of PMMA? *Polym. Degrad. Stab.* **2009**, *94*, 1298−1306.

(11) Wang, Q.; Undrell, J. P.; Gao, Y. S.; Cai, G. P.; Buffet, J. C.; Wilkie, C. A.; O'Hare, D. Synthesis of flame-retardant polypropylene/LDH-borate nanocomposites. *Macromolecules* **2013**, *46*, 6145−6150.

(12) Xu, W. Z.; Zhang, B. L.; Wang, X. L.; Wang, G. S.; Ding, D. The flame retardancy and smoke suppression effect of a hybrid containing CuMoO4 modified reduced graphene oxide/layered double hydroxide on epoxy resin. *J. Hazard. Mater.* **2018**, *343*, 364−375.

(13) Wang, D.; Mu, X. W.; Cai, W.; Zhou, X.; Song, L.; Ma, C.; Hu, Y. Nano-bridge effects of carbon nanotubes on the properties reinforcement of two-dimensional molybdenum disulfide/polymer composites. *Compos. A* **2019**, *121*, 36−44.

(14) Xu, Y. J.; Wang, J.; Tan, Y.; Qi, M.; Chen, L.; Wang, Y. Z. A novel and feasible approach for one-pack flame-retardant epoxy resin with long pot life and fast curing. *Chem. Eng. J.* **2018**, *337*, 30−39.

(15) Tan, Y.; Shao, Z. B.; Yu, L. X.; Xu, Y. J.; Rao, W. H.; Chen, L.; Wang, Y. Z. Polyethyleneimine modified ammonium polyphosphate toward polyamine-hardener for epoxy resin: thermal stability, flame retardance and smoke suppression. *Polym. Degrad. Stab.* **2016**, *131*, 62−70.
(16) Xu, Y. J.; Chen, L.; Rao, W. H.; Qi, M.; Guo, D. M.; Liao, W.; Wang, Y. Z. Latent curing epoxy system with excellent thermal stability, flame retardance and dielectric property. *Chem. Eng. J.* **2018**, *347*, 223−232.
(17) Wei, L. L.; Wang, D. Y.; Chen, H. B.; Chen, L.; Wang, X. L.; Wang, Y. Z. Effect of a phosphorus-containing flame retardant on the thermal properties and ease of ignition of poly (lactic acid). *Polym. Degrad. Stab.* **2011**, *96*, 1557−1561.
(18) Xu, W. Z.; Wang, S. Q.; Li, A. J.; Wang, X. L. Synthesis of aminopropyltriethoxysilane grafted/tripolyphosphate intercalated ZnAl LDHs and their performance in the flame retardancy and smoke suppression of polyurethane elastomer. *RSC Adv.* **2016**, *6*, 48189−48198.
(19) Shan, X. Y.; Song, L.; Xing, W. Y.; Hu, Y.; Lo, S. Effect of nickel-containing layered double hydroxides and cyclophosphazene compound on the thermal stability and flame retardancy of poly (lactic acid). *Ind. Eng. Chem. Res.* **2012**, *51*, 13037−13045.
(20) Qiu, S. L.; Xing, W. Y.; Feng, X. M.; Yu, B.; Mu, X. W.; Yuen, R. K.; Hu, Y. Self-standing cuprous oxide nanoparticles on silica@ polyphosphazene nanospheres: 3D nanostructure for enhancing the flame retardancy and toxic effluents elimination of epoxy resins via synergistic catalytic effect. *Chem. Eng. J.* **2017**, *309*, 802−814.
(21) Qiu, S. L.; Wang, X.; Yu, B.; Feng, X. M.; Mu, X. W.; Yuen, R. K.; Hu, Y. Flame-retardant-wrapped polyphosphazene nanotubes: A novel strategy for enhancing the flame retardancy and smoke toxicity suppression of epoxy resins. *J. Hazard. Mater.* **2017**, *325*, 327−339.
(22) Xu, G. R.; Xu, M. J.; Li, B. Synthesis and characterization of a novel epoxy resin based on cyclotriphosphazene and its thermal degradation and flammability performance. *Polym. Degrad. Stab.* **2014**, *109*, 240−248.
(23) Bai, Y. W.; Wang, X. D.; Wu, D. Z. Novel cyclolinear cyclotriphosphazene-linked epoxy resin for halogen-free fire resistance: synthesis, characterization, and flammability characteristics. *Ind. Eng. Chem. Res.* **2012**, *51*, 15064−15074.
(24) Sun, J.; Yu, Z. Y.; Wang, X. D.; Wu, D. Z. Synthesis and performance of cyclomatrix polyphosphazene derived from trispiro-cyclotriphosphazene as a halogen-free nonflammable material. *ACS Sustainable Chem. Eng.* **2014**, *2*, 231−238.
(25) Wu, C. C.; Wu, W. H.; Qu, H. Q.; Xu, J. Z. Synthesis of a novel phosphazene derivative and its application in intumescent flame retardant-EVA copolymer composites. *Mater. Lett.* **2015**, *160*, 282−285.
(26) Yang, G.; Wu, W. H.; Wang, Y. H.; Jiao, Y. H.; Lu, L. Y.; Qu, H. Q.; Qin, X. Y. Synthesis of a novel phosphazene-based flame retardant with active amine groups and its application in reducing the fire hazard of Epoxy Resin. *J. Hazard. Mater.* **2019**, *366*, 78−87.
(27) Guo, X.; Wang, H. S.; Ma, D. L.; He, J. N.; Lei, Z. Q. Synthesis of a novel, multifunctional inorganic curing agent and its effect on the flame-retardant and mechanical properties of intrinsically flame retardant epoxy resin. *J. Appl. Polym. Sci.* **2018**, *135*, 46410.
(28) Shi, L.; Li, D. Q.; Li, S. F.; Wang, J. R.; Evans, D. G.; Duan, X. Structure, flame retarding and smoke suppressing properties of Zn-Mg-Al-CO3 layered double hydroxides. *Chin. Sci. Bull.* **2005**, *50*, 1101−1104.
(29) Zhu, J.; Wu, Y.; Zhao, L.; Wei, H. L.; Chu, H. J.; He, J. Study of thermal properties of curing of DGEBA epoxy resin with Hexakis-(4-aminophenoxy)-cyclotriphosphazene. *Adv. Mater. Res.* **2011**, *284-286*, 365−368.
(30) Rives, V. Characterisation of layered double hydroxides and their decomposition products. *Mater. Chem. Phys.* **2002**, *75*, 19−25.
(31) Hong, N. N.; Song, L.; Wang, B. B.; Stec, A. A.; Hull, T. R.; Zhan, J.; Hu, Y. Co-precipitation synthesis of reduced graphene oxide/NiAl-layered double hydroxide hybrid and its application in flame retarding poly (methyl methacrylate). *Mater. Res. Bull.* **2014**, *49*, 657−664.
(32) Wen, T.; Wu, X. L.; Tan, X. L.; Wang, X. K.; Xu, A. W. One-pot synthesis of water-swellable Mg-Al layered double hydroxides and graphene oxide nanocomposites for efficient removal of As(V) from aqueous solutions. *ACS Appl. Mater. Interfaces* **2013**, *5*, 3304−3311.
(33) Zhao, S.; Xu, J. H.; Wei, M.; Song, Y. F. Synergistic catalysis by polyoxometalate-intercalated layered double hydroxides: oximation of aromatic aldehydes with large enhancement of selectivity. *Green Chem.* **2011**, *13*, 384−389.
(34) Krishnadevi, K.; Grace, A. N.; Alagar, M.; Selvaraj, V. Development of hexa(aminophenyl) cyclotriphosphazene- modified cyanate ester composites for high-temperature applications. *High Perform. Polym.* **2014**, *26*, 89−96.
(35) Wang, W.; Pan, H. F.; Shi, Y. Q.; Pan, Y.; Yang, W.; Liew, K. M.; Song, L.; Hu, Y. Fabrication of LDH nanosheets on β-FeOOH rods and applications for improving the fire safety of epoxy resin. *Compos. A* **2016**, *80*, 259−269.
(36) Matusinovic, Z.; Wilkie, C. A. Fire retardancy and morphology of layered double hydroxide nanocomposites: a review. *J. Mater. Chem.* **2012**, *22*, 18701−18704.
(37) Ma, W.; Xu, B.; Shao, L. S.; Liu, Y. T.; Chen, Y. J.; Qian, L. J. Synthesis of (1,4-Methylenephenylphosphinic acid) Piperazine and Its Application as a Flame Retardant in Epoxy Thermosets. *Macromol. Mater. Eng.* **2019**, *304*, No. 1900419.
(38) Wang, J. Y.; Xu, B.; Wang, X. D.; Liu, Y. T. A phosphorous-based bi-functional flame retardant for rigid polyurethane foam. *Polym. Degrad. Stabil.* **2021**, *186*, No. 109516.
(39) Zhou, K. Q.; Gao, R.; Qian, X. D. Self-assembly of exfoliated molybdenum disulfide (MoS_2) nanosheets and layered double hydroxide (LDH): towards reducing fire hazards of epoxy. *J. Hazard. Mater.* **2017**, *338*, 343−355.
(40) Xu, W. Z.; Wang, X. L.; Liu, Y. C.; Li, W.; Chen, R. Improving fire safety of epoxy filled with graphene hybrid incorporated with zeolitic imidazolate framework/layered double hydroxide. *Polym. Degrad. Stab.* **2018**, *154*, 27−36.
(41) Gann, R. G.; Babrauskas, V.; Peacock, R. D.; Hall, J. R., Jr. Fire conditions for smoke toxicity measurement. *Fire Mater.* **1994**, *18*, 193−199.
(42) Xu, W. Z.; Zhang, B. L.; Xu, B. L.; Li, A. J. The flame retardancy and smoke suppression effect of heptaheptamolybdate modified reduced graphene oxide/layered double hydroxide hybrids on polyurethane elastomer. *Compos. A* **2016**, *91*, 30−40.
(43) Li, Z.; Zhang, J. H.; Dufosse, F.; Wang, D. Y. Ultrafine nickel nanocatalyst-engineering of an organic layered double hydroxide towards a super-efficient fire-safe epoxy resin via interfacial catalysis. *J. Mater. Chem. A* **2018**, *6*, 8488−8498.
(44) Yuan, B. H.; Sun, Y. R.; Chen, X. F.; Shi, Y. Q.; Dai, H. M.; He, S. Poorly−/well-dispersed graphene: abnormal influence on flammability and fire behavior of intumescent flame retardant. *Compos. A* **2018**, *109*, 345−354.
(45) Zhao, S. J.; Yin, J. Y.; Zhou, K. Q.; Cheng, Y.; Yu, B. In situ fabrication of molybdenum disulfide based nanohybrids for reducing fire hazards of epoxy. *Compos. A* **2019**, *122*, 77−84.

https://doi.org/10.1021/acsomega.2c01719
ACS Omega 2022, 7, 21714−21726